Observation and Analysis of High Mass X-ray Binary (HMXB) Pulsars Cen X-3 and 2RXP J130159.6-635806.

Name: Ainsley Shamsuddin

Student number: 23332343

Date: 04/05/2025

Abstract

Cen X-3 and 2RXP J130159.6-635806 are known HMXB pulsars. This report uses XMM Newton data analysis techniques to study their behaviour in their respective binary systems. We look specifically at the emission of hard and soft x-rays for both systems and discuss the nature of the accretion in the systems. The lightcurve for Cen X-3 is structured enough to allow for further analysis in different epochs. The 2RXP J130159.6-635806 lightcurve is persistent and has distinct peaks and are related to the pulsars period. A theoretical model is also constructed using `xspec` to appropriately fit the data from these two sources.

Introduction

This report details the observation and the behaviour of eclipsing high mass X-ray pulsars in binary star systems. The data analysed is from the XMM Newton X-ray telescope observing the Cen X-3 pulsar in the V* V779 Cen binary system and the 2RXP J130159.6-635806 pulsar in the IGR J13020-6359 system. V* V779 Cen and IGR J13020-6359 are the optical designations of the binary system however they refer to the donor star specifically, as it is those stars who are optically dominant in the binary. PN and MOS1 were the main instruments used for the observations with ID 0111010101 for Cen X-3 and ID 0201920101 for 2RXP J130159.6-635806.

Cen X-3 is one of the first X-ray emitting pulsars to be discovered and studied. The Cen X-3 system comprises of a high energy compact neutron star (NS) and its O-type supergiant companion star also known as “Krzemiński's star” after Polish astronomer Wojciech Krzemiński. A special characteristic of Cen X-3 is its orientation in the galactic plane when observed from Earth. The Cen X-3 system is classified as an eclipsing binary system with one star (pulsar) passing in front and behind the other star (donor star) when observed. In this report, this binary system is studied specifically in the period where the neutron star emerges from an eclipse and emits soft and hard x-rays due to the overflow of the system’s Roche lobe [1]. The Roche lobe referred to is the gravitational territory of the donor star where its gravity has dominant control over the motion of the material in the system. As the star expands, material near the system’s inner Lagrangian point (L1) is no longer gravitationally bound. In such situations, the formation of an accretion disk is likely. Wind from the donor star is stored within this type of accretion structure and is able to flow smoothly into the poles of the orbiting NS. [1] Cen X-3 closely orbits its donor star with a period of 2.08 days and an eccentricity of < 0.0016 [2]. Due to its small orbital period and hence, a small orbital radius, a funnel point at L1 is formed which allows for the transfer of mass from the supergiant onto the neutron star. The x-rays detected by XMM Newton are generated due to the high temperatures created by this process. Most of this report will detail information about the Cen X-3 pulsar by looking at its periodicity and spectrum and comparing it with other research to ensure accuracy.

2RXP J130159.6-635806 is an accretion powered x-ray pulsar initially identified by INTEGRAL. After its detection by INTEGRAL, XMM Newton began following this x-ray pulsar in the years 2001-2004 since it was in its field of view. 2RXP J130159.6-635806 is reported to have a spin period of ~700 s and reside in the IGR J13020-6359 binary system [8]. For this observation, we aim to deduce the periodicity of this pulsar from the lightcurves and confirm it with literature values along with analysing and modelling its spectrum.

Methods

Observing the behaviour of Cen X-3 and 2RXP J130159.6-635806 involves several methods of data analysis. This section specifies the general methods used for data extraction, filtering, examination of x-ray lightcurves and the modelling of spectra. Specific details and reasoning for each step in the method are explained further in the results and analysis section.

To begin initial observations, the binary system is imaged from the raw data collected from XMM Newton and an unfiltered and filtered image is created. DS9 was the software used for this imaging. DS9 allows us to change colour filters to better see the shape of the system, scale the observation differently to see a larger view of the sky and select specific regions of space to observe. Creation of a filtered image allows us to crop a section of the observed sky, effectively discarding unwanted background photons around the binary system. X-ray photons of similar energies can also be categorised or "binned" together, allowing for further analysis which will be done in the next section. The `evselect` command is used in the creation of filtered images and tables.

Once we obtain a filtered image, we can begin lightcurve analysis by selecting the region we want to study. The information of the circular region can be obtained from DS9 and converted to physical units. This allows us to focus in on the source, ignoring the x-ray photons outside of the selected region. The `fv` program is used in visualising the overall lightcurve generated from the region. From this, additional filters can be added on such as time filters and ignoring specific count rates. Hard and soft x-ray lightcurve analysis is conducted using the `lcurve` command and the search for periodicity of the pulsar is done with the `efsearch` and `efold` commands.

Finally, the spectrum of the system can be plotted using `xspec`. Spectrum files, background files, ancillary file and photon redistribution matrix must be created first for `xspec` to analyse and model the data. These files give information about how the detector responds to photons of different energies and how effective it is at detecting those photons. The spectrum and its parameters are tweaked until a suitable model is obtained. The χ^2 value for each spectrum should aim to be close to unity indicating that the theoretical model is able to perfectly fit the data being analysed.

Results and analysis

Results from the 0111010101 observation (Cen X-3) is presented first followed by results from the 0201920101 observation (2RXP J130159.6-635806).

Cen X-3

Imaging and filtering the binary system

The `evselect` command was used to create an unfiltered image of the Cen X-3 binary system from the original data file obtained from XMM. This was done for both PN and MOS2 instruments.

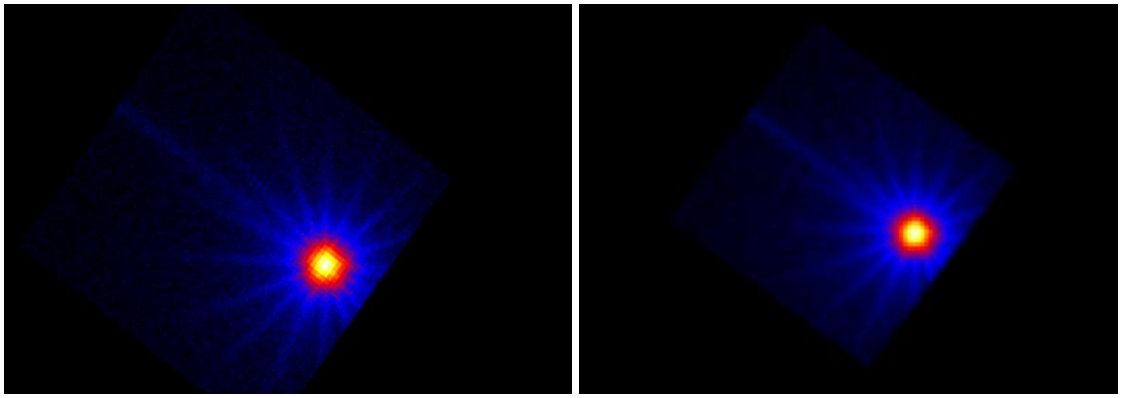

Fig 1. Cen X-3 binary comparison of the unfiltered image (left) and filtered image (right). Both taken using the PN instrument on XMM Newton with a colour filter on ds9.

The image above is the Cen X-3 system. When observed with XMM Newton, the binary is seen as a "point source" due to the brightness of the donor star dominating the system. As a result, XMM is unable to resolve both the pulsar and the donor star individually. The left image captures more x-ray photons which allows it to have a better spatial resolution than the image on the right.

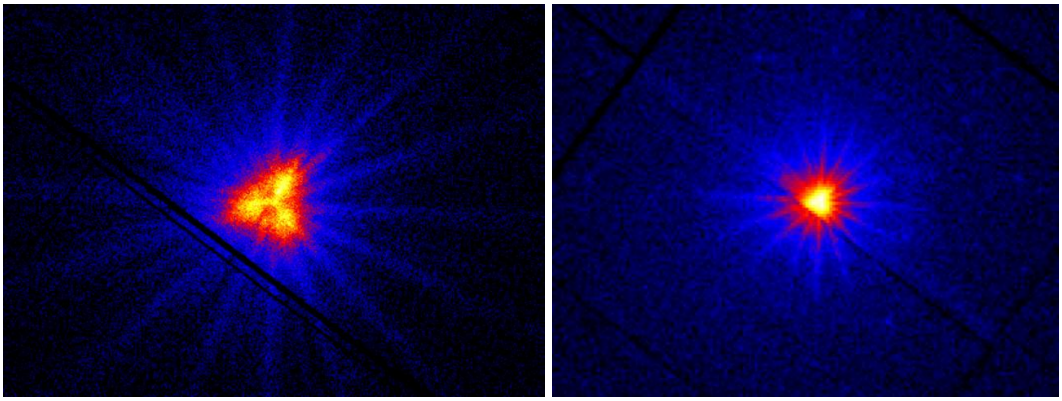

Fig 2. MOS2 images of the Cen X-3 binary system. Unfiltered image (left) and filtered image (right).

A comparison can be made between the observations generated by the PN instrument and the MOS2 instrument. MOS2's unfiltered image depicts a "triangular"-like x-ray source rather than a circular one when compared to PN. Some dark areas can be seen in the unfiltered MOS2 image which may be due to multiple high energy photons striking the detector causing photon pile up or it may be due to the effect of the telescope's point spread function [3]. In the case of photon pile up, the detector is unable to resolve them into individual photons and ends up detecting them as a single higher energy photon and discards them altogether creating a darker spot that we see in fig 2. The filtered image for MOS2 shows diffraction within the red and blue regions, whereas only the blue region is shown to diffract the most in the PN images. For this reason, the data collected from the PN instrument is likely better suited for further x-ray analysis.

Lightcurve analysis

We specifically look at the emission of the hard and soft x-rays from this source as it gives us information about the motion of the pulsar during its orbit around the companion star.

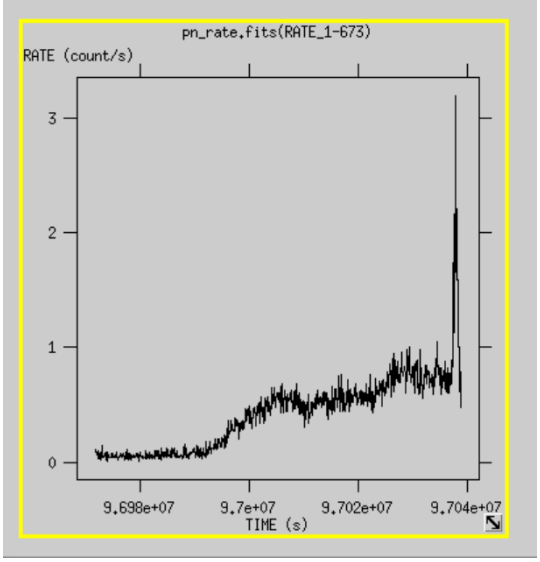

Fig 3. Initial plot of x-ray count rate vs time of the Cen X-3 eclipsing binary system.

A soft proton flare in the x-ray lightcurve at x = 9.704E+07 is seen occurring when the pulsar is fully out of eclipse. This does not originate from the Cen X-3 system but instead from the protons deflected into the detector by XMM's mirrors [4]. A time filter is applied to discard this interval as it does not contribute to our analysis.

Before focussing on the source, noisy background counts are removed to ensure we examine data related to the binary system with the least amount of noise as possible. A suitable count rate threshold is applied for PN (0.35 counts/s) and for MOS (0.4 counts/s) instruments.

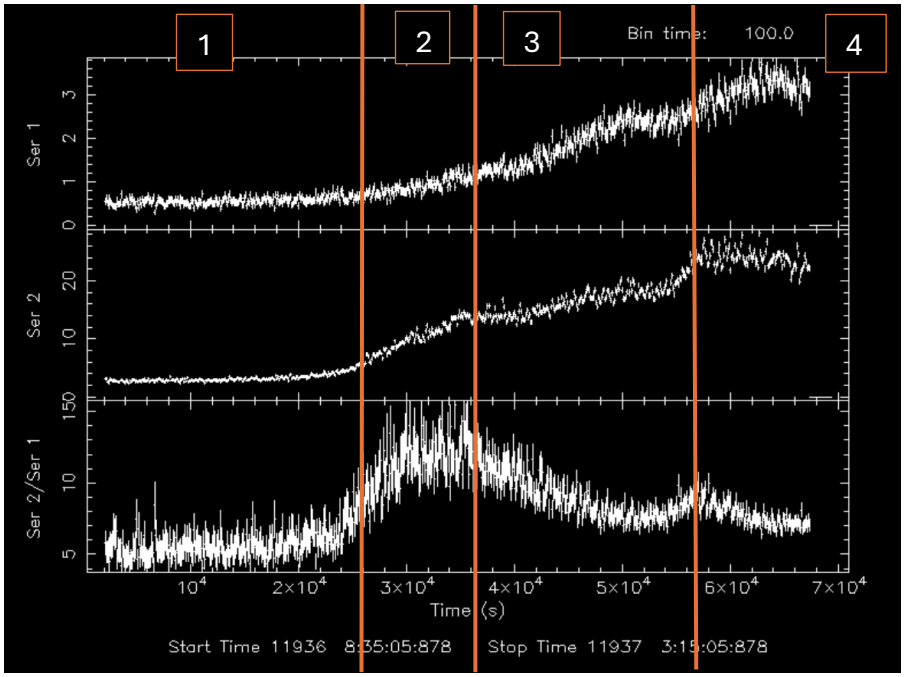

Fig 3. X-ray light curve of soft and hard x-rays split into four epochs to study the motion of the pulsar during the eclipse. Series 1: Soft x-rays, Series 2: Hard x-rays, Series 2/Series 1: Ratio of hard to soft x-rays.

Fig 3 was plotted using the `lcurve` command. It is split into hard and soft x-rays. This was done by changing the PI (the preferred pulse height of the event), using 300 – 2000 keV for soft x-rays and 2000-10000 keV for hard x-rays.

Epoch 1 is a stable and low x-ray emission period where the pulsar is behind its companion star (total eclipse). In epoch 2, the x-ray count in series 1 and series 2 begin to increase. The increase in x-ray counts suggest that the pulsar is beginning to emerge from the eclipse of the donor star. The hard x-ray counts tend to be higher than the soft x-ray counts in this epoch due to hard x-rays being highly energetic and are able to move through interstellar medium easier. A notable spike is seen in the hardness ratio graph (series 3) during epoch 2. The lower count rates for soft x-rays is likely due to photoelectric absorption during the eclipse event [1]. In epoch 3 there is steady rise in both x-ray counts signifying a bigger portion of the pulsar coming out of the eclipse. Finally, a flat but high count rate in epoch 4 suggests that the pulsar is now fully out of the eclipse.

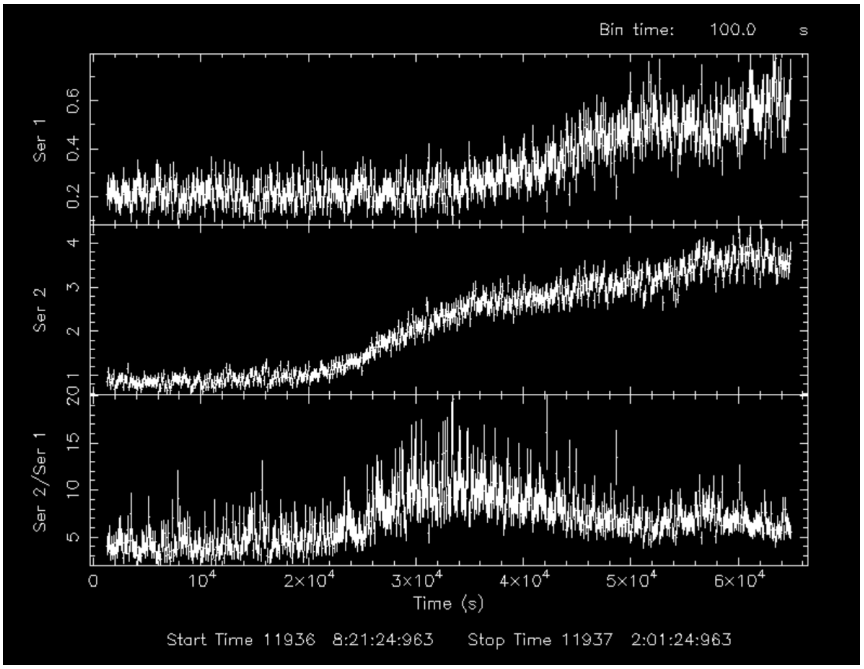

Fig 3.1. MOS2 x-ray light curve of Cen X-3. Series 1: Soft x-rays, Series 2: Hard x-rays, Series 3: Ratio of hard x-rays vs soft x-rays.

The plot of the lightcurves in fig 3.1 does not heavily differ from the fig 3 plot. Large vertical error bars are seen prominently in series 1 and 3 meaning that a significant amount of noise was detected by MOS2. Fig 3 and fig 3.1 comparison was made with other research of the Cen X-3 lightcurve data [1] and [5] to look for similarity.

Finding pulsations and the period of pulsations

We expect to find clear pulsations in epochs 3 and 4 as these are the main temporal regions where the pulsar emerges from the eclipse of the companion star. The clearest and most distinct pulsations of the pulsar are expected to be detected most accurately in epoch 4 since the entire pulsar is free from obstruction. Additionally, we also expect to see clear pulsations when looking specifically at hard x-rays since they are energetic enough to pierce interstellar obstructions such as dust more easily than soft x-rays. Below are the graphs obtained using the `efsearch` command when looking for pulsations in the x-ray lightcurve at different intervals.

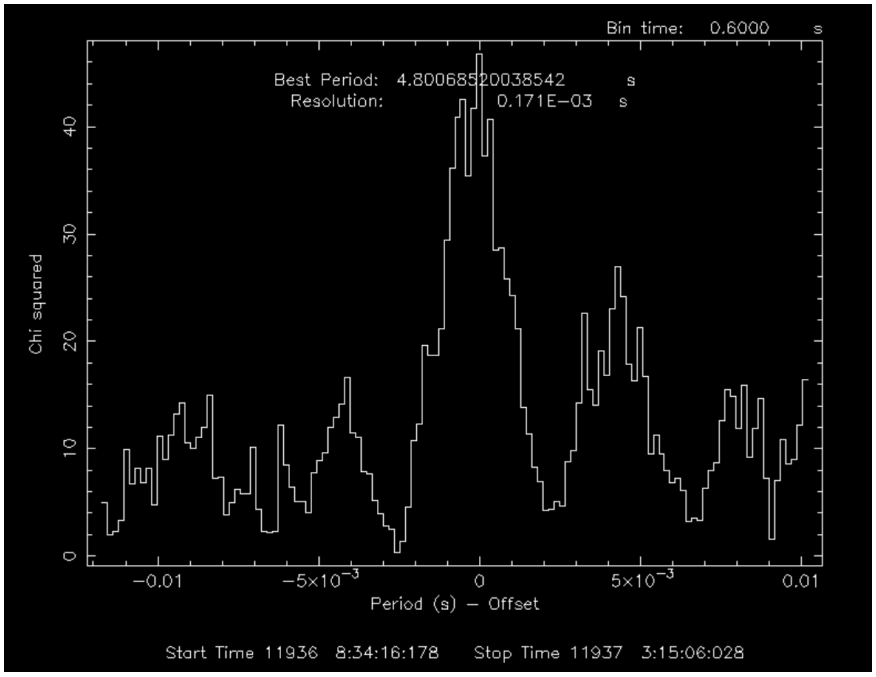

Fig 4. Interval 3 for hard x-rays measured using PN. The period estimation is accurate and is in line with the literature value of 4.8s. This plot begins to slowly resemble a gaussian distribution with some noise.

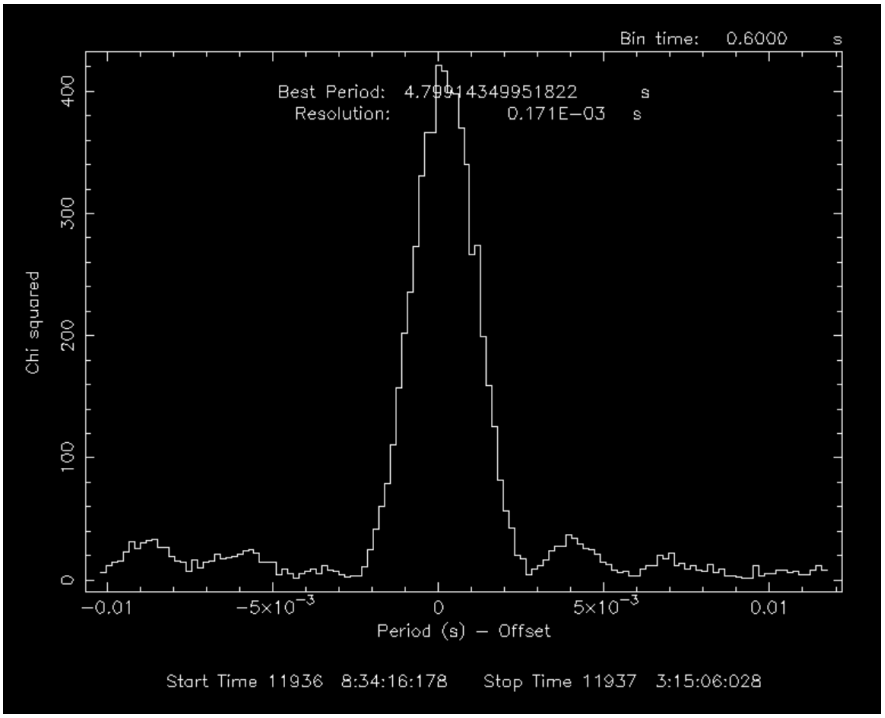

Fig 4.1 Epoch 4 - hard x-rays. This plot resembles a near perfect Gaussian distribution.

The Gaussian distribution resemblance allows us to conclude that the period is centred around a stable value of 4.8s with only a minor amount of deviation throughout the observation period.

To verify and see the period of pulsation more clearly, the **`efold`** command was used to fold the light curve, amplify observed pulsations and to check again the accuracy of the **`efsearch`** graphs in fig 4 and 4.1.

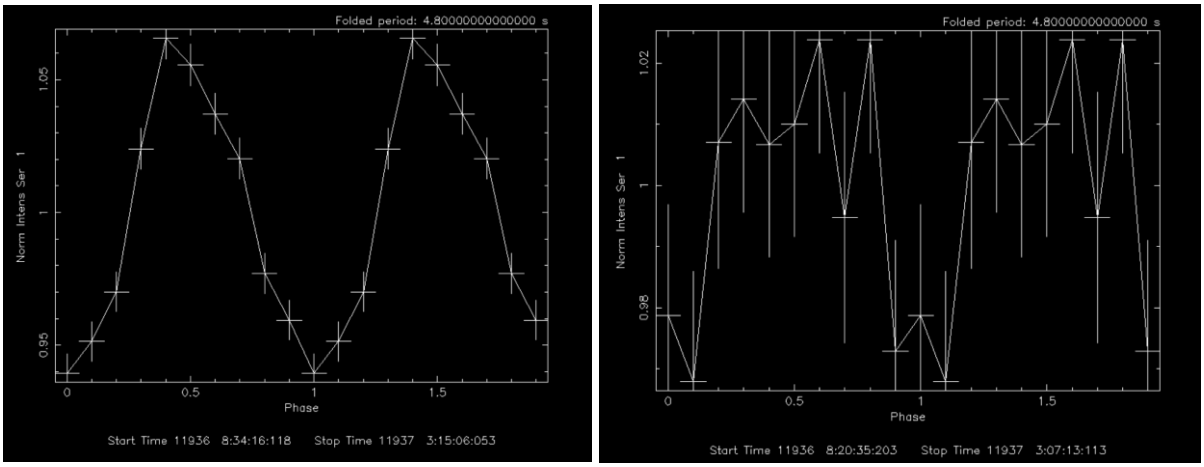

Fig 4.2. Folded light curve for the 4th epoch for hard x-rays. Left: PN, right: MOS2.

For the PN folded lightcurve, error bars are seen to be small and don't intersect in the region of other datapoints. The variation in the period is small which means that the data analysed is not affected much by noise. Asymmetrical peaks are present to better visualise the shape of the period. A period can be seen in the MOS2 graph however, error bars are comparatively larger than the PN graph and their shape is not identical. A reason for this could be due to the instrument's different temporal resolutions, MOS is in full frame mode and PN is in timing mode. [7] Fig 4.2 is added below to show the comparison of the folded lightcurve of hard x-rays and soft x-rays.

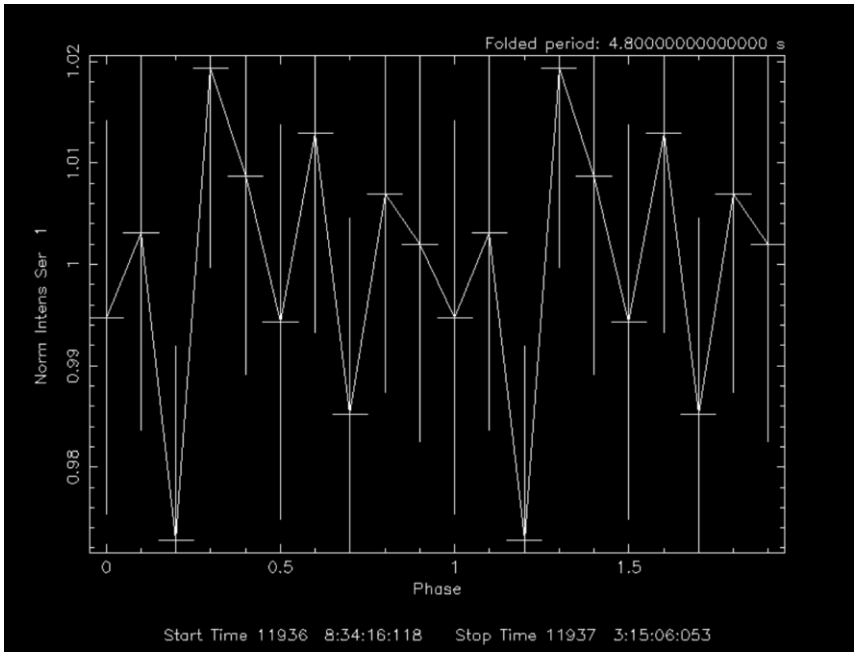

Fig 4.2 efold graph of soft x-rays in epoch 4.

No clear periodic pattern is seen,and error bars are large. Soft x-rays are prone to absorption and scattering due to the stellar wind of the donor star obscuring and scattering the soft x-ray photons, hence, creating non-periodic and random dips that are not actually related to the periodicity of the pulsar. [6]

Spectral analysis

A spectrum of count rates vs energy (keV) is plotted using `xspec` for Cen X-3. The model used was `wabs*(gaussian+bbody+powerlaw+gaussian).`

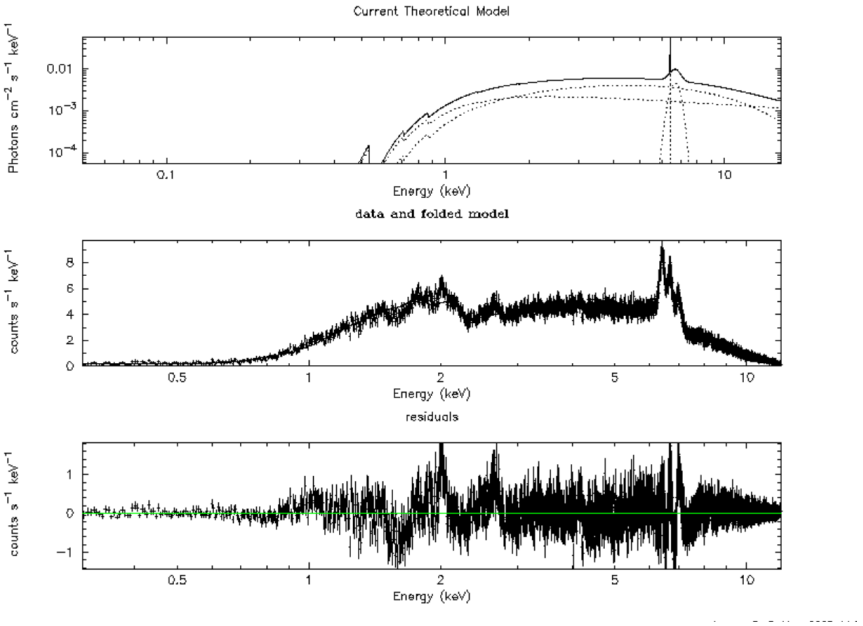

Fig 5. Plot of the overall Cen X-3 spectrum.

Table 1. Overall model parameters for the Cen X-3 spectrum.

#	Component	Parameter	Unit	Value	Uncertainty
1	wabs	nH	10^{22}	0.598728	± 0.0204756
2	gaussian	LineE	keV	6.67038	± 0.0699971
3	gaussian	Sigma	keV	0.271859	± 0.0675086
4	gaussian	norm	-	3.14865E-03	± 7.44388E-04
5	bbody	kT	keV	2.63097	± 0.0740635
6	bbody	norm	-	5.53393E-03	± 4.70004E-04
7	powerlaw	PhoIndex	-	0.412746	± 0.0790515
8	powerlaw	norm	-	3.64388E-03	± 2.59281E-04
9	gaussian	LineE	keV	6.39038	± 0.0227422
10	gaussian	Sigma	keV	4.33743E-05	± 2.34238E-05
11	gaussian	norm	-	7.23401E-04	± 3.67639E-04

χ^2 value: 3390

the nH parameter represents is the hydrogen column density, the number of hydrogen atoms in our line of sight per cm^2. If the value of nH is high, more x-rays are blocked. This can strongly affect soft x-rays, completely blocking some with lower energy levels out. nH is around 0.6×10^{22} for this spectrum (moderate blockage) so soft x-rays can still be detected.

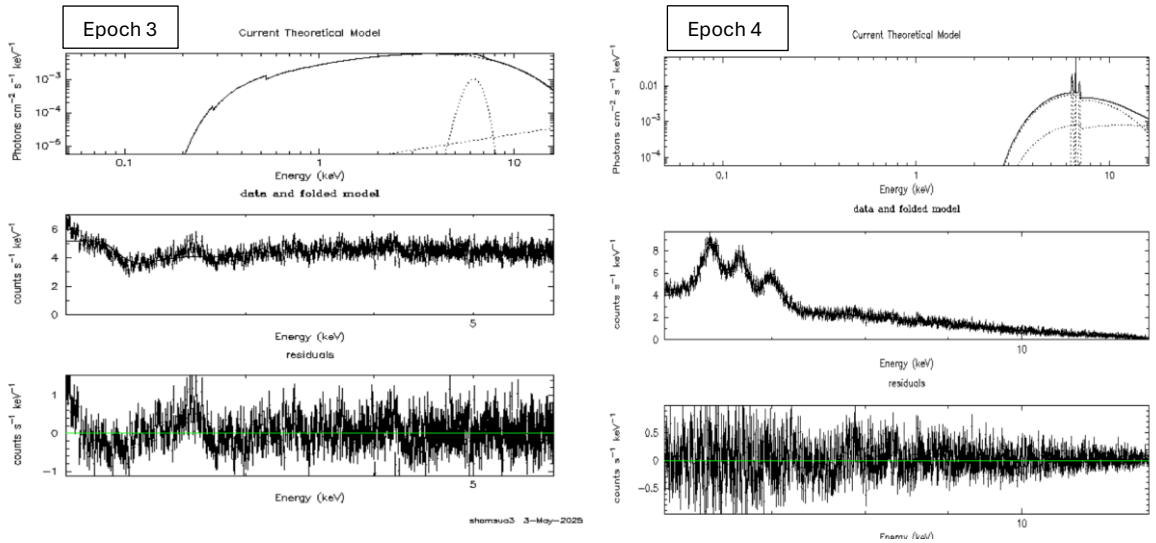

Fig 5.1 Spectrum of epochs 3 (2 keV – 6 keV) and 4 (6 keV – 12 keV) of Cen X-3.

Similar to the lightcurve analysis, the overall spectrum for Cen X-3 is divided into different epochs by ignoring specific energy values to see how well the theoretical model fits the data during the motion of the pulsar around the companion. The same model was used to model the spectrum for epochs 3 and 4. The overall model has a high χ^2 value and is not considered a good fit since χ^2 is not close enough to 1. However, when splitting the spectrum into different epochs the χ^2 value of the model is reduced with values 979.77 and 1209.67 respectively suggesting that the accuracy of the model becomes slightly better when looking at specific parts of the spectrum.

2RXP J130159.6-635806

A similar procedure to the Cen X-3 binary source was taken to analyse the 2RXP J130159.6-635806 source.

Imaging and filtering the binary system

MOS1 captures two binary systems, the inner system is a radio source (PSR B1259-63) and the outer system 2RXP J130159.6-635806. Images filtered using DS9 standard filters to better see the sources.

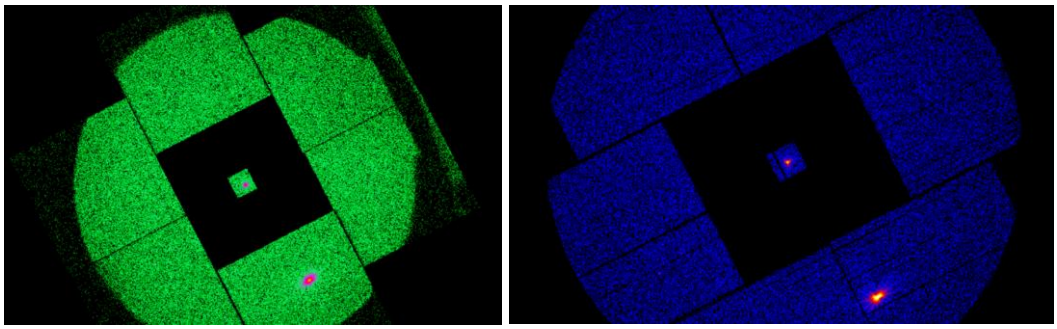

Fig 6. Filtered images of the PSR B1259-63 radio binary system and 2RXP J130159.6-635806. Left image: detected by MOS1 instrument, right image: detected by MOS2 instrument.

Lightcurve analysis

Below are the hard and soft x-ray lightcurves of 2RXP J130159.6-635806 constructed with `lcurve`.

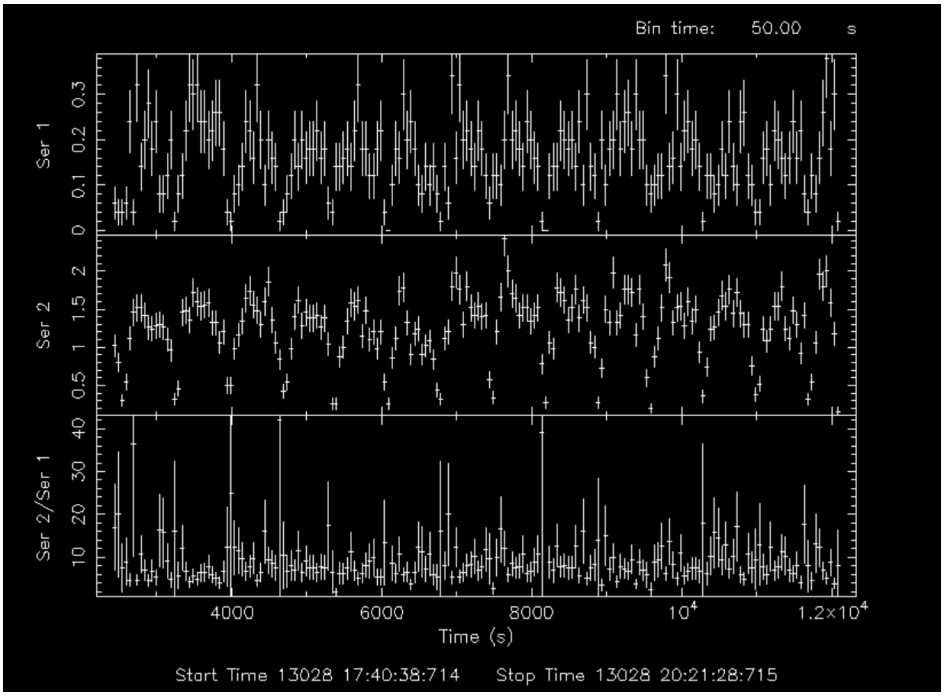

Fig 7. X-ray lightcurve of 2RXP J130159.6-635806. Series 1: soft x-rays, series 2: hard x-rays, series 3: ratio of hard x-rays to soft x-rays.

Notable pulsations can be seen in the lightcurve especially in series 2 (hard x-rays). 2RXP J130159.6-635806 has a period of 700 s. A bin time of 50s is used to better see the pulsations. A bin time of 100s would work well to observe the pulsation however there would be less plotted datapoints and visually, the pulsations in series 2 would be harder to make out. See fig 7.1 for comparison. The lightcurve datapoints in fig 7 are consistent indicating that during this observation period, the pulsar is not obscured by another object. Pulsars that have companion stars actively fill the Roche lobes often have much shorter spin periods, but this is not the case for 2RXP J130159.6-635806. Instead, it is likely that it orbits around a Be main sequence star [8].

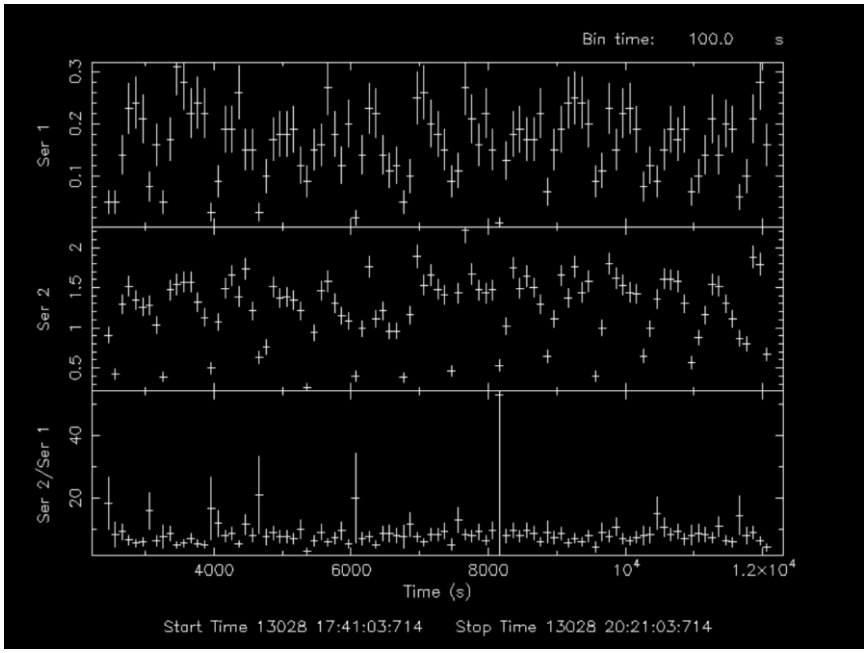

Fig 7.1 X-ray lightcurve of 2RXP J130159.6-635806 with time binning 100s for comparison. Series 1: soft x-rays, series 2: hard x-rays, series 3: ratio of hard x-rays to soft x-rays.

Finding pulsations and the period of pulsations

The `efsearch` and `efold` commands are used to identify clearly the pulsation period of 700s. The graphs below convey the same information however they are binned differently with different resolutions. The graph on the right allows us to clearly see more accurately the peaks occurring every 700s. The graph on the right shows us the pulsation behaviour over a larger time scale.

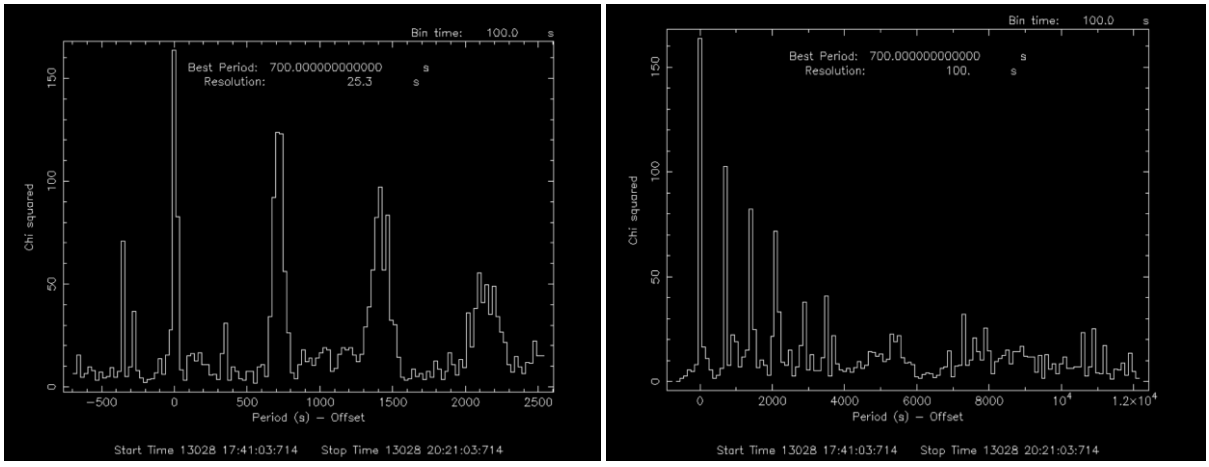

Fig 8. efsearch hard x-ray graphs to visualise periodic behaviour of 2RXP J130159.6-635806.

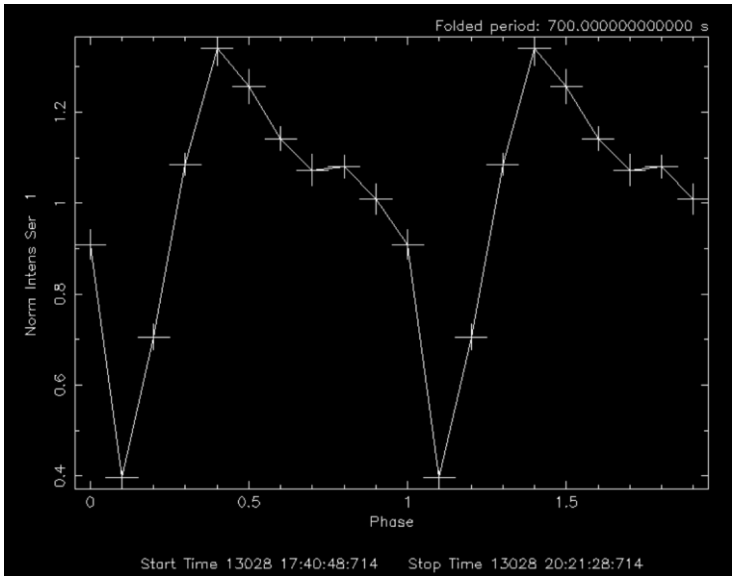

Fig 8.1. efold graph of hard x-rays for 2RXP J130159.6-635806.

A distinct periodic shape can be seen in the efold graph confirming the period to be 700 seconds.

Modelling the spectrum using xpsec

The figure and table below show the results of the spectrum analysis of 2RXP J130159.6-635806.

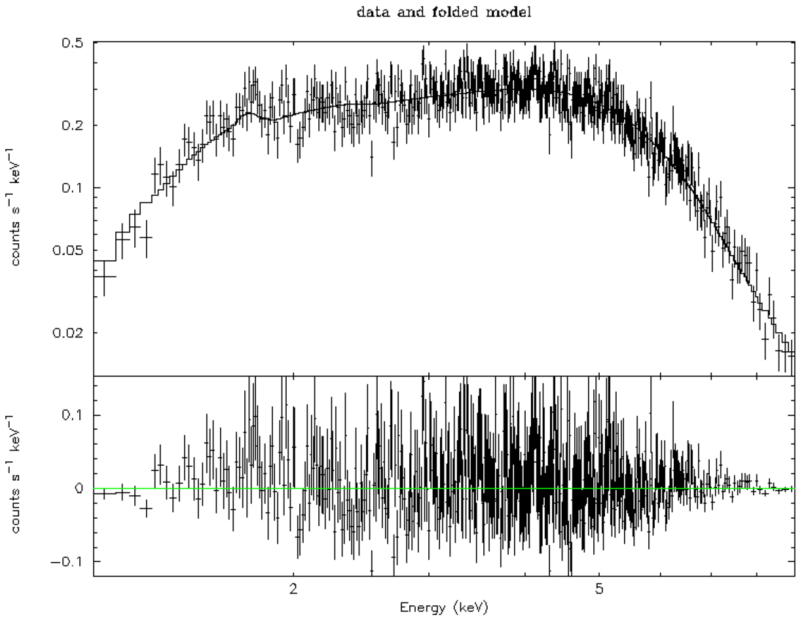

Fig 9. Overall spectral plot of the data and the residual.

The model uses a combination of models specifically `wabs*(bbody+gaussian+logpar)` to achieve a χ^2 value of 405.04. Since the spectrum is plotted in the log scale, the `logpar` model seemed fitting to add as it may help in getting a more accurate fit for the spectrum. However, this model is not a perfect model since χ^2 is not near unity. The residual plot in fig 9 shows a wide spread of deviation suggesting that this model is only a rough approximation of the source.

Table 2. Model parameters for 2RXP J130159.6-635806 spectrum.

No.	Model Component	Parameter	Unit	Value	± Error
1	wabs	nH	10^{22}	3.24535	± 0.458211
2	bbody	kT	keV	0.26068	± 0.058774
3	bbody	norm	—	0.173192	± 0.117103
4	gaussian	LineE	keV	3.33717	± 0.736630
5	gaussian	sigma	keV	1.9436	± 0.802163
6	gaussian	norm	—	1.82170	± 1.06828
7	logpar	alpha	—	4.0000	± 13.7427
8	logpar	beta	—	1.32196	± 5.06353
9	logpar	pivotE	(scale)	50.0000	(fixed)
10	logpar	norm	—	5.75995e-05	± 3.15414e-05

The model uses a combination of models specifically `wabs*(bbody+gaussian+logpar)` to achieve a χ^2 value of 405.04. Since the spectrum is plotted in the log scale, the `logpar` model seemed fitting to add as it may help in getting a more accurate fit for the spectrum. However, this model is not a perfect model since χ^2 is not 1. The residual plot in fig 9 shows a wide spread of deviation suggesting that this model is only a rough approximation of the source.

Conclusion

Image, lightcurve and spectral analysis was done on Cen X-3 and 2RXP J130159.6-635806. Both are x-ray pulsars that reside in binary systems. In our observation, the motion of Cen X-3 was studied before, during and after its egress of the companion star. Analysing the soft and hard x-ray photon emission led us to conclude that Cen X-3 has periodic pulsations of 4.8 seconds which aligns with literature values. The same analysis was done with the 2RXP J130159.6-635806 source. It was found that 2RXP J130159.6-635806 has a period of 700 s and its pulsations can be seen in the lightcurve itself. Spectra models were created to model both sources. Generally, the χ^2 values were high for both models however they were seen to decrease when splitting the spectrum into different epoch and apply the model to each.

References

[1] Sanjurjo-Ferrín, Graciela, et al. "X-ray variability of the HMXB Cen X− 3: evidence for inhomogeneous accretion flows." Monthly Notices of the Royal Astronomical Society 501.4 (2021): 5892-5909.

[2] https://gammaray.msfc.nasa.gov/gbm/science/pulsars/lightcurves/cenx3.html

[3] https://svi.nl/Point-Spread-Function-%28PSF%29

[4] https://xmm-tools.cosmos.esa.int/external/xmm_user_support/documentation/uhb/epicextbkgd.html

[5] A.V.Tugay, A.A Vasylenko. "XMM-Newton Observations of X-ray Pulsar Cen X-3". YSC'16 Proc. of Contributed Papers, eds.: Choliy V.Ya., Ivashchenko G., Kyivskyi Universitet, Kyiv, p. 58-61, 2009

[6]M.C Ramadevi, JRF. Space Astronomy and Instrumentation Division. ISRO Satellite Centre. https://web.iucaa.in/~dipankar/ph217/contrib/xrb.pdf

[7] A.M. Read, M. Guainazzi, and S. Sembay. Cross-calibration of the XMM-Newton EPIC pn and MOS on-axis effective areas using 2XMM sources.

[8] M. Chernyakova, A. Lutovinov, J. Rodríguez, M. Revnivtsev, Discovery and study of the accreting pulsar 2RXP J130159.6-635806, Monthly Notices of the Royal Astronomical Society, Volume 364, Issue 2, December 2005, Pages 455–461, https://doi.org/10.1111/j.1365-2966.2005.09548.x //2RXP J130159.6-635806